Eidgenössische Technische Hochschule Zürich
Ecole polytechnique fédérale de Zurich
Politecnico federale di Zurigo
Swiss Federal Institute of Technology Zurich

Extrusion contraction upwind schemes for convection-diffusion problems

H. Heumann and R. Hiptmair

Research Report No. 2008-30
October 2008

Seminar für Angewandte Mathematik
Eidgenössische Technische Hochschule
CH-8092 Zürich
Switzerland

Extrusion contraction upwind schemes for convection-diffusion problems

Holger Heumann, Ralf Hiptmair

October 13, 2008

Abstract

The calculus of differential forms allows to state general convection-diffusion problems using the notion of Lie derivatives. We apply the Cartan formula for Lie derivatives and the contraction extrusion dualism to propose an upwind discretization procedure based on discrete differential forms. We discuss this procedure in detail for 0-forms and the scalar convection-diffusion boundary value problem. In the case of linear ansatz spaces one of the stable schemes derived with this procedure coincides with Tabata's upwind scheme. In the case of quadratic ansatz spaces we get a new scheme that enjoys stability properties similar to SUPG.

1 Introduction

The discretization of boundary value problems for the singularly perturbed convection-diffusion equation

$$-\varepsilon\Delta u + \nabla u \cdot \boldsymbol{\beta} = f \quad \text{in } \Omega \subset \mathbb{R}^n \ , \tag{1}$$

has attracted and continues to attract much attention in numerical analysis. The main difficulty are challenging stability issues connected with steep characteristic or boundary layers of the solution. This manifests itself as spurious solutions produced by standard methods.

Motivated by the maximum principle that holds for solutions of the continuous equation, stable discretization schemes are achieved by ensuring that the discrete solution operator L_h is inverse monotone. Examples are one sided upwind finite differences, the upwind finite element methods discussed in Ikeda [15] or the nonlinear finite elements scheme of Mizukami and Hughes [18]. All these methods establish matrix representations $\boldsymbol{A}$ of L_h that are of positive type (i.e., $a_{ii} > 0$, $a_{ij} \leq 0$, if $i \neq j$, and $a_{ii} \geq \sum_{j\neq i} a_{ij}$). Similar to Godunov's result for the time dependent transport equation, a finite difference method with this property is at most first-order consistent [23]. Nevertheless Roos [19] describes a family of second-order consistent finite difference methods in one dimension that have inverse monotone matrix representations. Using a result of Lorenz [17], he showed that they are a product of inverse monotone matrices. Unfortunately this technique is not applicable for finite difference methods in two or higher dimensions. Besides this there are several attempts to define a proper discrete maximum principle for the finite element context [9].

Another family of discretization methods, mainly based on finite elements or the discontinuous Galerkin approach adds some mesh dependent terms to the standard formulation to control the gradient of the solution independently of the diffusion constant ε. Representatives of this family are SUPG [6], GLSFEM [14] or methods using interior penalty terms [7].

A new perspective is adopted in this paper. We start from the observation that (1) is just one specific instance of a larger family of boundary value problems modeling convective phenomena, including e.g. magnetic convection. The calculus of differential forms permits us to express the governing partial differential equation as

$$-\varepsilon d * d\omega + *L_{\boldsymbol{\beta}}\omega = \varphi \quad \text{in } \Omega \subset \mathbb{R}^n \ . \tag{2}$$

This is an equation for an unknown l-form ω, $0 \leq l \leq n$. The symbol $*$ stands for the so-called Hodge operator mapping an l-form to an $n-l$-form, and d denotes the exterior derivative. Together they define the principal part $d * d\omega$ of the differential operator. Differential forms can be modelled by means of functions and vector fields through so-called vector proxies [5, page 132]. For $n = 3$, in the case of $*$ induced by the Euclidean metric on $\mathbb{R}^3$, the operator $*d\omega$ becomes $-\Delta$, $\nabla \times (\nabla \times \cdot)$, and $\nabla \cdot \nabla$ in vector proxy notation, for $l = 0, 1, 2$, respectively. We refer to [12] for more details and an introduction to the calculus of differential forms.

Thinking in terms of differential forms offers considerable advantages as regards the construction of structure preserving spatial finite element discretizations of boundary value problems for $d{*}d\omega$: one can devise discrete counterparts of l-forms defined on triangulations of Ω, which provide suitable piecewise polynomial finite element spaces for the variational problems arising from $d * d\omega$. In particular, discrete differential forms respect the algebraic properties of the exterior derivative like $d^2 = 0$ and the DeRham exact sequence. More details are given in [2, 5, 13]. Discrete differential forms of any polynomial degree are available [1, 11]. In light of the success of discrete differential forms, it is worth exploring their use for the more general equation (2).

The convective part of the operator from (2) is formulated by means of the Lie derivative $L_{\boldsymbol{\beta}}$, where $i\boldsymbol{\beta}$ is a vector field on Ω. Thus, for $l = 0$ and in terms of vector proxies, (2) becomes (1). As explained by Bossavit in [3], the Lie derivative operator itself is a composition of the so called contraction operators $i_{\boldsymbol{\beta}}$ and the exterior derivatives. The definition of the contraction is based on the notion of extrusion of manifolds and the duality pairing of forms and manifolds [4]. This characterization perfectly matches the approximation techniques based on discrete differential forms.

However, an ambiguity due the discontinuity of discrete differential forms needs to be handled in the extrusion contraction discretization of $L_{\boldsymbol{\beta}}$. We propose to use this to incorporate an *upwinding aspect* into the discretization of convective terms. We show, that this procedure applied to the scalar equation, that is, the case of 0-forms, not only reproduces Tabata's upwind scheme [22], but yields other consistent schemes that are more stable than the standard scheme. We even derive a new scheme for second order Lagrangian elements, that seems to be comparable stable with a SUPG scheme. This is independent of the mesh orientation and there is no specific parameter to be choosen.

We first review the definition of Lie derivatives and contraction via the extrusion of manifolds. Next, we propose an approximation procedure for contraction operators of arbitrary discrete l-forms. Together with the exterior derivative and discrete Hodge operators this gives an approximation for general convection-diffusion boundary value problems. We illustrate the construction for the case of 0-forms. The schemes will depend on the choice of a quadrature rule and an interpolation operator. We give sufficient conditions on the parameters of the schemes to preserve the convergence rates for the second order part and use these to derive different schemes for linear and quadratic ansatz spaces. Finally we present numerical experiments, that show that our approximation procedure leads to superior stability properties.

1.1 Extrusion, Contraction and Lie derivatives

We write $\mathcal{D}^l$ for the space of l-forms on Ω. The Lie derivative $L_{\boldsymbol{\beta}}$ of a l-form $\omega \in \mathcal{D}^l$ is the generalization of the directional derivative for a scalar function $u \in \mathcal{D}^0$:

$$(\boldsymbol{\beta} \cdot \boldsymbol{\nabla} u)(\boldsymbol{x}) := \lim_{\substack{t \to 0 \\ >}} \frac{u(\boldsymbol{s}_t(\boldsymbol{x})) - u(\boldsymbol{s}_0(\boldsymbol{x}))}{t}. \tag{3}$$

Here $\boldsymbol{s}_t$ is a parameter dependent family of diffeomorphisms $\boldsymbol{s}_t : \Omega \mapsto \Omega$ that generates the integral curves of the velocity field $\boldsymbol{\beta}$. For differential forms $\omega \in \mathcal{D}^l$ of order l, $l > 0$, we replace the point evaluation of 0-form u with integration over l-dimensional oriented sub-manifolds M_l of Ω. To emphasize the duality of differential l-forms ω_l and l-dimensional oriented manifolds we introduce the notation

$$< \omega_l, M_l > := \int_{M_l} \omega_l \ .$$

Then the Lie derivative of a l-form ω is:

$$< L_{\boldsymbol{\beta}}\omega, M_l > := \lim_{\substack{t \to 0 \\ >}} \frac{< \omega, \boldsymbol{s}_t(M_l) > - < \omega, M_l >}{t}, \tag{4}$$

where $\boldsymbol{s}_t(M_l)$ is a short notation for the union of points on flux lines emerging from M_l at fixed t. Following [4] we introduce the extrusion $Ext_t(\boldsymbol{\beta}, M_l) = \{\boldsymbol{s}_\tau(\boldsymbol{x}_0) : 0 \leq \tau \leq t, \, \boldsymbol{x}_0 \in M_l\}$ as the union of flux lines emerging at M_l running from 0 to t (Figure 1). We define an orientation of the extrusion $Ext_t(\boldsymbol{\beta}, M_l)$ such that

$$\partial Ext_t(\boldsymbol{\beta}, M_l) = \boldsymbol{s}_t(M_l) - M_l - Ext_t(\boldsymbol{s}_t, \partial M_l). \tag{5}$$

Plugging this into the definition of the Lie derivative (4) we get by means of Stokes theorem

$$\begin{aligned} < L_{\boldsymbol{\beta}}\omega, M_l > &= \lim_{\substack{t \to 0 \\ >}} \frac{< \omega, \partial Ext_t(\boldsymbol{\beta}, M_l) > + < \omega, Ext_t(\boldsymbol{\beta}, \partial M_l) >}{t} \\ &= \lim_{\substack{t \to 0 \\ >}} \frac{< \mathrm{d}\omega, Ext_t(\boldsymbol{\beta}, M_l) > + < \omega, Ext_t(\boldsymbol{\beta}, \partial M_l) >}{t}. \end{aligned} \tag{6}$$

Remark 1.1 *For smooth differential forms we have*

$$L_{-\boldsymbol{\beta}} = -L_{\boldsymbol{\beta}} \ . \tag{7}$$

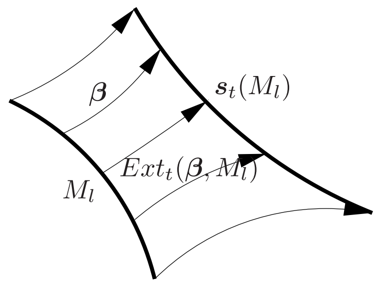

Figure 1: Extrusion of line segment M_l with respect to velocity field $\boldsymbol{\beta}$.

The contraction operator is defined as the limit of the dual of the extrusion:

$$< i_{\boldsymbol{\beta}}\omega, M_l >:= \lim_{\substack{t \to 0 \\ >}} \frac{< \omega, Ext_t(\boldsymbol{\beta}, M_l) >}{t} \tag{8}$$

and we recover from (6) the Cartan magic formula [16, page 142, prop. 5.3] for the Lie derivative:

$$< L_{\boldsymbol{\beta}}\omega, M_l >=< i_{\boldsymbol{\beta}}\mathrm{d}\omega, M_l > + < \mathrm{d}i_{\boldsymbol{\beta}}\omega, M_l > . \tag{9}$$

For 0-forms the second term vanishes, for top forms the first one.

Remark 1.2 *For* 1*-forms with vector proxy* $\mathbf{A}$ *in* $\mathbb{R}^3$ *this gives a general convective term*

$$L_{\boldsymbol{\beta}}\mathbf{A} \sim \boldsymbol{\beta} \times \boldsymbol{\nabla} \times \mathbf{A} + \boldsymbol{\nabla}(\boldsymbol{\beta} \cdot \mathbf{A}) .$$

We refer to [3] for vector proxy representations Lie derivatives of other forms on two and tree dimensional manifolds.

1.2 Discrete Contraction and Lie derivative

Write $\mathcal{W}^l \subset \mathcal{D}^l$ for some space of discrete l-forms on a triangulation of Ω [13]. The properties of discrete differential forms ensure that exterior derivatives map discrete forms on discrete forms. By virtue of (9), this means that an approximation of the contraction operator already yields discrete Lie derivatives.

We propose the following procedure. We introduce auxiliary spaces $\mathcal{W}^{l,i} \subset \mathcal{D}^l(\Omega)$ of discrete differential forms with basis functions $(b_i^l)_{i=1\ldots N_l} \in \mathcal{W}^{l,i}$ such that all global degrees of freedom $(l_i^l)_{i=1\ldots N_l}$ are integral evaluations $l_i^l(\cdot) :=< \cdot, M_l^i >$ on l dimensional oriented manifolds M_l^i. Due to the non smoothness of discrete differential forms we have in general

$$l_i^l(i_{\boldsymbol{\beta}}\omega_h) \neq -l_i^l(i_{-\boldsymbol{\beta}}\omega_h)$$

for $\omega_h \in \mathcal{W}^{l+1}$. Hence we do not expect to preserve the linearity of Lie derivatives in $\boldsymbol{\beta}$ as in the smooth case (see Remark 1.1). Here we propose an approximation of the contraction operator $i_{\boldsymbol{\beta}}\omega_h \in \mathcal{D}^l(\Omega)$, that complies with the successful upwind idea from the finite difference method:

Definition 1.3 *Given a discrete interpolation space $\mathcal{W}^{l,i} \subset \mathcal{D}^l$ with basisfunction $(b_i^l)_{i=1\dots N_l} \in \mathcal{W}^{l,i}$ and global degrees of freedom $l_i^l(\cdot) :=< \cdot, M_l^i >$ the* upwind interpolation *$I^l(i_{\boldsymbol{\beta}}\omega_h)$ of the contraction of a $(l+1)$-form $\omega_h \in \mathcal{W}^{l+1}$ is defined as*

$$I^l(i_{\boldsymbol{\beta}}\omega_h) = \sum_{i=1}^{N_l} -l_i^l(i_{-\boldsymbol{\beta}}\omega_h)b_i^l. \tag{10}$$

This is indeed an upwind method since we use only information from the upwind direction:

$$-l_i^l(i_{-\boldsymbol{\beta}}\omega_h) \quad = \quad -\lim_{\substack{t \to 0 \\ >}} < \omega_h, Ext_t(-\boldsymbol{\beta}, M_l^i) > . \tag{11}$$

As exterior derivatives map discrete forms on discrete forms the operator

$$L_{\boldsymbol{\beta}}^h\omega_h := I^l(i_{\boldsymbol{\beta}}d\omega) + dI^{l-1}(i_{\boldsymbol{\beta}}\omega_h) \tag{12}$$

is well defined for $\omega_h \in \mathcal{W}^l$. Then discrete Hodge operators $*_h$ [12] yield discrete counterparts

$$b_h(\omega_h, \nu_h) :=< *_h L_{\boldsymbol{\beta}}^h\omega_h, \nu_h > \tag{13}$$

of the bilinear form

$$b(\omega_h, \nu_h) =< *L_{\boldsymbol{\beta}}\omega_h, \nu_h > . \tag{14}$$

on $\mathcal{W}^l \times \mathcal{W}^l$. At first glance it seems to be crude to approximate Lie derivatives via upwind interpolation of the contractions. But we presume that the consistency of the approximation depends only on additional conditions on the interpolation spaces and the discrete Hodge operators. Moreover we expect good stability properties of the resulting schemes due to the upwinding present in the discretizations. Below we investigate these issues for the simplest case of 0-forms in two dimensions.

2 Extrusion contraction upwinding for 0-forms

0-forms are scalar functions u and their Lie derivatives are the streamline derivatives

$$L_{\boldsymbol{\beta}}u = \boldsymbol{\beta} \cdot \boldsymbol{\nabla} u. \tag{15}$$

To illustrate the proposed approximation procedure for Lie derivatives (i.e. convective terms) based on interpolation of contraction and discrete Hodge operators we will discuss in the following several discretizations of the standard convection-diffusion problem:

$$\begin{aligned} -\varepsilon\Delta u(\mathbf{x}) + \boldsymbol{\beta}(\mathbf{x}) \cdot \boldsymbol{\nabla} u(\mathbf{x}) &= f(\mathbf{x}) \qquad \text{on } \Omega \subset \mathbf{R}^2 \\ u(\mathbf{x}) &= g(\mathbf{x}) \qquad \partial\Omega, \end{aligned}$$

where we assume that $\varepsilon > 0$ and $\boldsymbol{\beta}$ continuous with $\|\boldsymbol{\beta}\| = 1$. Hence we need to discretize the following weak formulation:

$$a(u, v) + b(u, v) = \langle l, v\rangle, \qquad u, v \in H_0^1(\Omega) \tag{16}$$

with the diffusion term

$$a(u, v) = \varepsilon \int_\Omega \boldsymbol{\nabla} u \cdot \boldsymbol{\nabla} v \,\mathrm{d}x, \tag{17}$$

and the convection term

$$b(u, v) = \int_\Omega \boldsymbol{\beta} \cdot \boldsymbol{\nabla} u\, v. \tag{18}$$

The convection term (18) is the realization of the bilinear form (14) for 0-forms.

We introduce a triangulation τ_h of the domain and define the usual piecewise polynomial approximation spaces $\mathcal{W}_k^0 = \{v \in C(\Omega), \forall T \in \tau, v|_T \in P_k(T)\} \subset H_0^1(\Omega)$. $P_k(T)$ is the set of polynomials with degree less or equal p. The approximated solution $u_h \in \mathcal{W}_k^0$ then fulfils

$$a(u_h, v_h) + b(u_h, v_h) = (f, v_h) \quad v_h \in \mathcal{W}_k^0. \tag{19}$$

To convert this equation in the unkown u_h into a system of equations for the expansion coefficients of u_h we approximate the convection term (18), either by one of the new upwind schemes or by the standard finite element Galerkin approach.

2.1 Upwind and standard approximation of the convection term

The definition (1.3) of the interpolation operator I^0 hinges on global degrees of freedom that are point evaluations. This leaves little choice for a basis of a interpolation space $\mathcal{W}^{0,i} \subset \mathcal{D}^0$. The second step in the approximation of (14) is the discrete Hodge $*_h$. Here we take for simplicity local quadrature rules $Q(T) = \{(\mathbf{x}_i^T, w_i^T)\}_{i=1\ldots N}$ defined on triangles $T \in \tau_h$ to approximate the L^2 innerproducts

$$(u_h, v_h)_T := \int_T u_h v_h \mathrm{d}x, \quad u_h \in \mathcal{W}^{0,i}, v_h \in \mathcal{W}_h^k$$

with

$$(u_h, v_h)_{T,h} := \sum_{i=1}^N (u_h v_h)(\mathbf{x}_i^T) w_i^T.$$

For a fixed quadrature $Q(T)$ and basis $(\tilde{b}_j)_{j=1\ldots M}$ of $\mathcal{W}^{0,i}$ the bilinear form (14) has the following representation:

$$\begin{aligned} b_h(u_h, v_h) &= (I^0(\boldsymbol{\beta} \cdot \boldsymbol{\nabla} u_h), v_h)_{\Omega,h} \\ &= \sum_{j=1}^M (\boldsymbol{\beta} \cdot \boldsymbol{\nabla} u_h|_{T_j})(\mathbf{x}_j) \sum_T \sum_{k=1}^N \tilde{b}_j(\mathbf{x}_k^T) v_h(\mathbf{x}_k^T) w_k^T. \end{aligned} \tag{20}$$

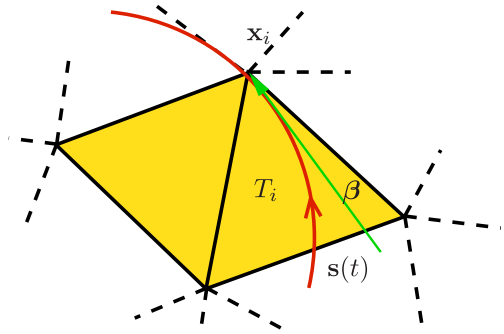

Figure 2: Streamline derivative and extrusion contraction characterization. T_i is the triangle in upwind direction.

The coefficients $(\boldsymbol{\beta} \cdot \boldsymbol{\nabla} u_h|_{T_j})(\mathbf{x}_j)$ here correspond to the upwind evaluations (11) of the global degrees of freedom $l_j^0(v_h) = v_h(\mathbf{x}_j)$. They depend on the restriction of $\boldsymbol{\beta} \cdot \boldsymbol{\nabla} u_h$ to that triangle T_j adjacent to interpolation point $\mathbf{x}_j$ that lies in upwind direction (see fig. 2). The standard finite element method in contrast uses only a local quadrature $Q_s(T) = \{(\mathbf{x}_i^T, w_i^T)\}_{i=1\dots N_s}$ to approximate the convection term (18) of the weak formulation (16):

$$b_h^s(u_h, v_h) \quad := \quad \sum_T \sum_{i=1}^{N_s} (\boldsymbol{\beta} \cdot \boldsymbol{\nabla} u_h)(\mathbf{x}_i^T) v_h(\mathbf{x}_i^T) w_i^T . \tag{21}$$

In order to compare both approximations we change the order of summation in (20), yielding

$$b_h(u_h, v_h) \quad = \quad \sum_T \sum_{i=1}^{N} \sum_{j=1}^{M} (\boldsymbol{\beta} \cdot \boldsymbol{\nabla} u_h|_{T_j})(\mathbf{x}_j) \tilde{b}_j(\mathbf{x}_i^T) v_h(\mathbf{x}_i^T) w_i^T . \tag{22}$$

If the restriction of the basis $(\tilde{b}_j)_{j=1\dots M}$ of $\mathcal{W}^{0,i}$ on a triangle T has N non–vanishing elements $\tilde{b}_{j_1}, \dots \tilde{b}_{j_N}$ such that $\tilde{b}_{j_k}(\mathbf{x}_i^T) = \delta_{ik}$ (22) is simplified as

$$b_h(u_h, v_h) \quad = \quad \sum_T \sum_{i=1}^{N} (\boldsymbol{\beta} \cdot \boldsymbol{\nabla} u_h|_{T_i})(\mathbf{x}_i^T) v_h(\mathbf{x}_i^T) w_i^T . \tag{23}$$

We recover the standard approximation (21) if none of the quadrature points is located on the boundary of a element.

2.2 Consistency error

If we use local polynomial basis functions of degree k and the standard approximation (21) to solve (19) the Strang lemma [10, Theorem 26.1] and consistency error estimates tell us, that the local quadrature rule must be exact for polynomials of degree $2k - 2$ [10, Theorem 29.1] to preserve the optimal convergence rates $O(h^k)$ for uniform h–refinement. Assuming that the interpolation I^0 in definition (1.3) is local we get a similar result for the new scheme (22).

Proposition 2.1 *We make the following assumptions on the interpolation I^0 from definition (1.3) and the local quadrature $Q(T)$:*

- *I^0 is local, e.g. for $v \in C^0(\Omega)$:*

$$v|_{\Omega_T} \equiv 0 \quad \Rightarrow \quad I^0(v)|_T \equiv 0,$$

where Ω_T is the union of all triangles T_i adjacent to T.

- *There exists $p \in \mathbb{N}$, such that for all triangles T*

$$I^0|_T(v) - Id|_T(v) = 0 \quad \forall v \in P_p(\Omega_T),$$

i.e. for all polynomials v of degree less or equal p on Ω_T.

- *$Q(T)$ is exact for polynomials of degree less or equal $(k+l)$.*

Then the consistency error $R(u_h, v_h) := |b(v_h, w_h) - b_h(v_h, w_h)|$ due to the approximation

$$b_h(u_h, v_h) = (I^0(\boldsymbol{\beta} \cdot \boldsymbol{\nabla} u_h), v_h)_{\Omega,h}, \quad u_h, v_h \in \mathcal{W}_k^0$$

defined in (20) is bounded

$$R(u_h, v_h) = |b(u_h, v_h) - b_h^e(u_h, v_h)| \leq Ch^{m+1} \|u_h\|_{m+1} \|v_h\|_1 \tag{24}$$

with C independent of the mesh and $m = \min(p, l)$. We denote with $\|\cdot\|_{s,D}$ and $\|\cdot\|_{s,\infty,D}$ the norms on Sobolev spaces $W^{s,2}(D)$ and $W^{s,\infty}(D)$ on some domain $D \subset \Omega$ and omit D if $D = \Omega$.

Proof: We follow the usual localization technique:

$$R(v_h, w_h) = \sum_T E_{\Omega_T}(\boldsymbol{\beta} \cdot \boldsymbol{\nabla} v_h, w_h)$$

with local error function:

$$E_{\Omega_T}(\boldsymbol{\beta} \cdot \boldsymbol{\nabla} v_h, w_h) := (\boldsymbol{\beta} \cdot \boldsymbol{\nabla} v_h, w_h)_T - (I^0(\boldsymbol{\beta} \cdot \boldsymbol{\nabla} v_h), w_h)_{T,h}.$$

Using the linear pullback $\boldsymbol{x} = \boldsymbol{B}_T \hat{\boldsymbol{x}} + \boldsymbol{b}_T$ to a reference triangle $\hat{T}$ we get the following relation

$$E_{\Omega_T}(\psi, \phi) = |\det \boldsymbol{B}_T| E_{\Omega_{\hat{T}}}(\hat{\psi}, \hat{\phi})$$

between E_{Ω_T} and the error $E_{\Omega_{\hat{T}}}(\hat{\psi}, \hat{\phi})$ on the reference element. Furthermore we have

$$E_{\Omega_{\hat{T}}}(\hat{\psi}, \hat{\phi}) = 0$$

for $\hat{\phi} \in P_k(\hat{T})$ and $\hat{\psi} \in P_m(\Omega_{\hat{T}})$. On the other hand

$$\begin{aligned} E_{\Omega_{\hat{T}}}(\hat{\psi}, \hat{\phi}) &\leq C\,\|\hat{\psi}\|_{0,\infty,\Omega_{\hat{T}}} \|\hat{\phi}\|_{0,\hat{T}} \\ &\leq C\,\|\hat{\psi}\|_{m+1,\infty,\Omega_{\hat{T}}} \|\hat{\phi}\|_{0,\hat{T}} \end{aligned}$$

for any $\hat{\psi} \in W^{m+1,\infty}(\Omega_{\hat{T}})$ and $\hat{\phi} \in P_k(\hat{T})$. Here we used the continuous embedding $W^{m+1,\infty} \hookrightarrow C^0$ and equivalence of norms in finite dimensional spaces. This shows that for fixed $\hat{\phi} \in P_k(\Omega_{\hat{T}})$ the functional

$$\hat{\psi} \rightarrow E_{\Omega_{\hat{T}}}(\hat{\psi}, \hat{\phi})$$

is a continuous linear functional which vanishes for $\hat{\psi} \in P_m(\Omega_{\hat{T}})$. Therefor we can apply the Bramble-Hilbert lemma and bound the error by the semi norm

$$E_{\Omega_{\hat{T}}}(\hat{\psi}, \hat{\phi}) \quad \leq \quad C\,|\hat{\psi}|_{m+1,\infty,\Omega_{\hat{T}}} \|\hat{\phi}\|_{0,\hat{T}}.$$

Choose now $\hat{\psi} = \hat{\mathbf{b}}\hat{\boldsymbol{\sigma}}$, $\hat{\mathbf{b}} \in (W^{m+1,\infty}(\Omega_{\hat{T}}))^2$, $\hat{\boldsymbol{\sigma}} \in (P_m(\Omega_{\hat{T}}))^2$, using the chain rule and the equivalence of norms again gives

$$E_{\Omega_{\hat{T}}}(\hat{\psi}, \hat{\phi}) \quad \leq \quad C \sum_{i=1}^{2} \sum_{j=0}^{m} |\hat{b}_i|_{m+1-j,\infty,\Omega_{\hat{T}}} |\hat{\sigma}_i|_{j,\Omega_{\hat{T}}} \|\hat{\phi}\|_{0,\hat{T}}.$$

Next we use scaling inequalities to obtain a bound for the error E_{Ω_T}:

$$\begin{aligned} E_{\Omega_T}(\psi, \phi) \quad &\leq \quad C h_T^{m+1} \sum_{i=1}^{2} \sum_{j=0}^{m} |b_i|_{m+1-j,\infty,\Omega_T} |\sigma_i|_{j,\Omega_T} \|\phi\|_{0,T} \\ &\leq \quad C h_T^{m+1} \sum_{i=1}^{2} \|b_i\|_{m+1,\infty,\Omega_T} \|\sigma_i\|_{m,\Omega_T} \|\psi\|_{0,T}. \end{aligned}$$

Replacing σ_i with $\partial_i v_h$, b_i with β_i and ϕ with w_h we arrive at:

$$E_{\Omega_T}(\boldsymbol{\beta} \cdot \boldsymbol{\nabla} v_h, w_h) \leq C\, h_T^{m+1}\, (\sum_{i=1}^{2} |\beta_i|_{m+1,\infty,\Omega_T}) \|v_h\|_{m+1,\Omega_T} \|w_h\|_{0,T}.$$

The Cauchy-Schwarz inequality finishes the proof provide the number of triangles in Ω_T is bounded.

■

Proposition 2.1 together with the Strang lemma [10, Theorem 26.1] gives sufficient conditions on the two building blocks interpolation I^0 and local quadrature $Q_c(T)$ in (20) to preserve the optimal order of convergence, i.e. k for the energy norm when $u_h, v_h \in \mathcal{W}_k^0$ in (19). If we limit the choice of an interpolation space $\mathcal{W}^{0,i}$ to the piecewise polynomial spaces $\mathcal{W}_p^0$ we have to ensure that for a fixed ansatz space $\mathcal{W}_k^0$ and a quadrature $Q(T)$ exact for $P_{k+l}(T)$ we have $\min(p, l) \geq k-1$. Since we want to keep the calculation as cheap as possible one would prefer choices of p and l with $p = l = k-1$. We will see that for stability reasons it is worth to slightly increase p. In order to better distinguish these new schemes we introduce the following notation for the approximation (20):

Definition 2.2 *Given an interpolation space $\mathcal{W}^{0,i} = \mathcal{W}_p^0$ with basis $(\tilde{b}_j)_{j=1\ldots M}$ and global degrees of freedom $(l_j^0)_{j=1\ldots M}$, that are point evaluations $l_j(\tilde{b}_k) := \tilde{b}_k(\mathbf{x}_j) = \delta_{kj}$ and a local quadrature $Q_c(T) = \{(\mathbf{x}_i, w_i^T)\}_{i=1\ldots N_c}$ we define:*

$$\begin{aligned} b_h^{p,c}(u_h, v_h) \quad &:= \quad (I_p^0(\boldsymbol{\beta} \cdot \boldsymbol{\nabla} u_h), v_h)_{\Omega, h_c} \\ &:= \quad \sum_{j}^{M} (\boldsymbol{\beta} \cdot \boldsymbol{\nabla} u_h|_{T_j})(\mathbf{x}_j) \sum_{T} \sum_{i=1}^{N_c} \tilde{b}_j(\mathbf{x}_i^T) v_h(\mathbf{x}_i^T) w_i^T \end{aligned} \tag{25}$$

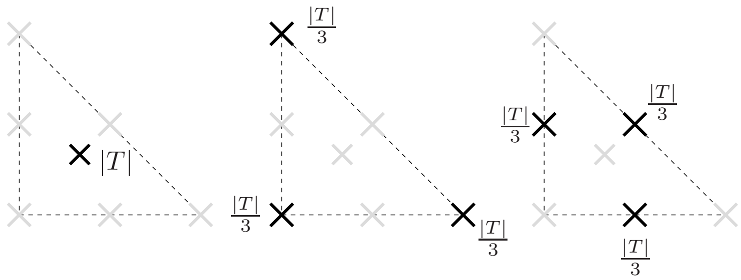

Figure 3: Location and weight of the quadrature points of the barycenter rule Q_T, the vertex rule Q_v and the midpoint rule Q_m.

Remark 2.3 *Proposition 2.1 includes the statement that a quadrature rule should be exact for polynomials of degree* $2k-1$. *This could be improved to* $2k-2$ *with a technical refinement of the proof based on insertion of projections due to Ciarlet [10, page 207]. The same technique is applicable for* L^2 *error estimates.*

2.3 Low order approximation

When we choose $k=1$ in (19) and conforming Lagrangian linear basis functions λ_i we need to ensure that $\min(p,l) \geq 0$. The cheapest method preserving the order of convergence uses piecewise constant interpolation I_0^0 in the characteristic functions ξ_T of triangles T of τ_h,

$$I_0^0(\boldsymbol{\beta} \cdot \boldsymbol{\nabla} u_h) := \sum_T (\boldsymbol{\beta} \cdot \boldsymbol{\nabla} u_h)(\mathbf{b}_T)\xi_T$$

and the barycenter quadrature rule $Q_b(T) = \{(\mathbf{b}_T, |T|)\}$, for $\mathbf{b}_T$ barycenter of T (see Fig. (3)):

$$b_h^{0,b}(u_h, v_h) = \sum_T (\boldsymbol{\beta} \cdot \boldsymbol{\nabla} u_h)(\mathbf{b}_T) v_h(\mathbf{b}_T)|T|.$$

Since we evaluate the contraction inside the elements this scheme does not include upwinding. This changes if we take $\mathcal{W}_1^0$ as interpolation space as well. Then we use the extrusion contraction characterization of the streamline derivative and at vertices $\mathbf{a}_i$ we take the value from the upwind direction $(\boldsymbol{\beta} \cdot \boldsymbol{\nabla} u_h|_{T_i})(\mathbf{a}_i)$, where T_i is the triangle in upwind direction at $\mathbf{a}_i$ (fig. 2). The interpolation operator reads:

$$I_1^0(\boldsymbol{\beta} \cdot \boldsymbol{\nabla} u_h) = \sum_{\mathbf{a}_i} (\boldsymbol{\beta} \cdot \boldsymbol{\nabla} u_h|_{T_i})(\mathbf{a}_i)\lambda_i \tag{26}$$

and the scheme is:

$$b_h^{1,b}(u_h, v_h) = \sum_{\mathbf{a}_i} (\boldsymbol{\beta} \cdot \boldsymbol{\nabla} u_h|_{T_i})(\mathbf{a}_i) \sum_{T : \mathbf{a}_i \in \bar{T}} \frac{|T|}{3} v_h(\mathbf{b}_T). \tag{27}$$

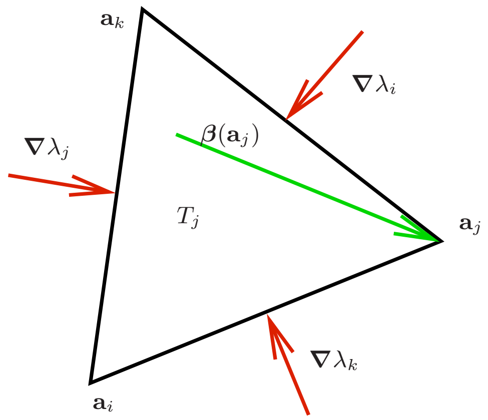

Figure 4: Sign condition for expansion coefficients of $I_1^0\boldsymbol{\beta}\cdot\boldsymbol{\nabla}\lambda$

Another local quadrature rule exact for $P_1(T)$ is the vertex rule (fig. (3))

$$Q_v(T) = \{(\mathbf{a}_{i_1}, \frac{|T|}{3}), (\mathbf{a}_{i_2}, \frac{|T|}{3}), (\mathbf{a}_{i_3}, \frac{|T|}{3})\}$$

evaluating the integrand at the three vertices $\mathbf{a}_{i_1}, \mathbf{a}_{i_2}, \mathbf{a}_{i_3}$ of a triangle T. While for piecewise constant interpolation the schemes using $Q_b(T)$ and $Q_v(T)$ coincide:

$$b_h^{0,v}(u_h, v_h) \quad = \quad b_h^{0,b}(u_h, v_h), \tag{28}$$

the scheme

$$b_h^{1,v}(u_h, v_h) = \sum_{\mathbf{a}_i} (\boldsymbol{\beta}\cdot\boldsymbol{\nabla} u_h|_{T_i})(\mathbf{a}_i) \sum_{T:\mathbf{a}_i\in\bar{T}} \frac{|T|}{3} v_h(\mathbf{a}_i) \tag{29}$$

differs from $b^{1,b}(u_h, v_h)$. The scheme $b^{1,v}(u_h, v_h)$ is exactly the scheme introduced by Tabata [22]. The crucial observation here is the sign property of the expansion coefficients $c_{ij} := (\boldsymbol{\beta}\cdot\boldsymbol{\nabla}\lambda_j|_{T_i})(\mathbf{a}_i)$ of the interpolation $I_1^0(\boldsymbol{\beta}\cdot\boldsymbol{\nabla}\lambda_j)$ (26). We have that $c_{ii} > 0$ and $c_{ij} \leq 0$, whenever $i \neq j$ (fig. 4). Thanks to the orthogonality $\lambda_i(\mathbf{a}_j) = \delta_{ij}$ of basis functions and quadrature points in (29) this sign property is inherited by the discrete matrix operator. The sign condition ensures that the corresponding discrete matrix operator is inverse monotone. Under mild additional assumptions one could prove that this scheme is L^∞ stable, uniformly in the diffusion constant ε [20, page 208].

When we combine the linear interpolation I_1^0 with the third order midpoint quadrature rule (fig. (3))

$$Q_m(T) = \{(\mathbf{m}_{\mathbf{e}_1}, \frac{|T|}{3}), (\mathbf{m}_{\mathbf{e}_2}, \frac{|T|}{3}), (\mathbf{m}_{\mathbf{e}_3}, \frac{|T|}{3})\}$$

based on evaluations at the midpoints $\mathbf{m}_{\mathbf{e}_k} = \frac{1}{2}(\mathbf{a}_{i_l} + \mathbf{a}_{i_m})$, for $\{k, l, m\}$ permutations of $\{1, 2, 3\}$, the interpolation remains the only approximation in $b_h^{1,m}(u_h, v_h)$.

Finally, we may also use second order Lagrangian elements as interpolation space. The basis functions are the quadratic polynomials $b_i^v = \lambda_i(2\lambda_i - 1)$ connected to vertices $\mathbf{a}_i$ and $b_{\mathbf{e}}^m = 4\lambda_{e_1}\lambda_{e_2}$ connected to midpoints $\mathbf{m}_{\mathbf{e}}$ of edges $\mathbf{e} = (e_1, e_2)$ between vertices $\mathbf{a}_{e_1}$ and $\mathbf{a}_{e_2}$. Hence we apply

$$I_2^0(\boldsymbol{\beta} \cdot \boldsymbol{\nabla} u_h) = \sum_{\mathbf{a}_i} (\boldsymbol{\beta} \cdot \boldsymbol{\nabla} u_h|_{T_i})(\mathbf{a}_i) b_i^v + \sum_{\mathbf{m}_{\mathbf{e}}} (\boldsymbol{\beta} \cdot \boldsymbol{\nabla} u_h|_{T_{\mathbf{e}}})(\mathbf{m}_{\mathbf{e}}) b_{\mathbf{e}}^m$$

to define $b_h^{2,b}(u_h, v_h)$, $b_h^{2,v}(u_h, v_h)$ and $b_h^{2,m}(u_h, v_h)$. With $b_h^{2,ex}(u_h, v_h)$ we want to denote an approximation using some quadrature rule that is exact for polynomials of degree 3. We could invent many more approximations using other quadrature rules or higher order interpolation operators.

2.4 Second order Lagrangian elements

In principle we could use all the approximations from the previous section for second order Lagrangian elements. In order to have consistent schemes that preserve the order of convergence proposition 2.1 tells us, that we need to consider more accurate quadrature rules. A combination of $Q_b(T)$ and $Q_v(T)$ gives a 4 point quadrature rule

$$Q_{vb}(T) = \{(\mathbf{a}_{i_1}, \frac{1}{12}|T|), (\mathbf{a}_{i_2}, \frac{1}{12}|T|), (\mathbf{a}_{i_3}, \frac{1}{12}|T|), (\mathbf{b}_T, \frac{3}{4}|T|)\}$$

of order 3, while a combination of $Q_b(T)$, $Q_v(T)$ and $Q_m(T)$ results in a 7 point quadrature rule

$$\begin{aligned} Q_{vmb}(T) = \quad & \{(\mathbf{a}_{i_1}, \frac{1}{20}|T|), (\mathbf{a}_{i_2}, \frac{1}{20}|T|), (\mathbf{a}_{i_3}, \frac{1}{20}|T|), \\ & (\mathbf{m}_{\mathbf{e}_1}, \frac{2}{15}|T|), (\mathbf{m}_{\mathbf{e}_2}, \frac{2}{15}|T|), (\mathbf{m}_{\mathbf{e}_3}, \frac{2}{15}|T|), (\mathbf{b}_T, \frac{9}{20}|T|)\} \end{aligned}$$

of order 4. These yield the approximations $b_h^{1,vb}(u_h, v_h)$ and $b_h^{2,vmb}(u_h, v_h)$. Additionally we apply some quadrature that evaluates the inner products of the quadratic basis functions exact to define $b_h^{2,ex}(u_h, v_h)$.

Based on the characterization of (22) as *upwind quadrature* we use $Q_{vb}(T)$ and $Q_{vmb}(T)$ to define a second family of approximations, which does not exactly fit into the framework of proposition 2.1 and definition 2.2

$$\begin{aligned} b_h^{1b,vb}(u_h, v_h) \quad &= \quad \sum_{\mathbf{a}_i} (\boldsymbol{\beta} \cdot \boldsymbol{\nabla} u_h|_{T_i})(\mathbf{a}_i) \sum_{T:\mathbf{a}_i \in T} \frac{|T|}{12} v_h(\mathbf{a}_i) \\ & \quad + \sum_T \frac{3}{4}|T| (\boldsymbol{\beta} \cdot \boldsymbol{\nabla} u_h)(\mathbf{b}_T) v_h(\mathbf{b}_T), \\ b_h^{2b,vmb}(u_h, v_h) \quad &= \quad \sum_{\mathbf{a}_i} (\boldsymbol{\beta} \cdot \boldsymbol{\nabla} u_h|_{T_i})(\mathbf{a}_i) \sum_{T:\mathbf{a}_i \in T} \frac{|T|}{20} v_h(\mathbf{a}_i) \\ & \quad + \sum_{\mathbf{m}_{\mathbf{e}}} (\boldsymbol{\beta} \cdot \boldsymbol{\nabla} u_h|_{T_i})(\mathbf{m}_{\mathbf{e}}) \sum_{T:\mathbf{m}_{\mathbf{e}} \in T} \frac{2}{15}|T| v_h(\mathbf{m}_{\mathbf{e}}) \\ & \quad + \sum_T \frac{9}{20}|T| (\boldsymbol{\beta} \cdot \boldsymbol{\nabla} u_h)(\mathbf{b}_T) v_h(\mathbf{b}_T). \end{aligned}$$

Nevertheless it is straightforward to show consistency in adapting the proof of proposition 2.1. The interpolation spaces $\mathcal{W}^{0,i}$ that correspond to these approximations are piecewise constant on meshes that are somehow dual to the initial tetrahedral mesh. The basis functions of $\mathcal{W}^{0,i}$ are the characteristic functions of cells attached to vertices, midpoints and barycenters and partitioning the triangles T adequate. The dual grid for $b_h^{1b,vb}(u_h, v_h)$ e.g. consists of cells surrounding the vertices and the barycenters of the initial triangulation. The overlap of a vertex cell of the dual grid and a triangle T is $\frac{1}{12}|T|$. That of a barycenter cell is $\frac{3}{4}|T|$.

3 Numerical experiments

3.1 Convergence

First we study the convergence rates for the various discretizations introduced in the previous section. We consider the convection-diffusion problem:

$$\begin{aligned} -\varepsilon\Delta u + 2\partial_x u + 3\partial_y u &= f \quad \text{in} \quad [0,1]^2 \\ u(x,y) &= g(x,y) \quad \text{in} \quad \partial[0,1]^2, \end{aligned} \tag{30}$$

where we chose f and g such that the solution is:

$$u(x,y) = xy^2 - y^2 e^{2\frac{x-1}{\varepsilon}} - xe^{3\frac{y-1}{\varepsilon}} + e^{2\frac{x-1}{\varepsilon}+3\frac{y-1}{\varepsilon}}. \tag{31}$$

Figures (5) and (6) confirm the statements of proposition 2.1. For linear ansatz spaces convergence in the energy norm is linear, while for quadratic polynomials the convergence is quadratic. We further stress that the approximation $b^{2,m}(u_h, v_h)$ preserves the convergence rate according to remark 2.3. If we measure the error in the L^2–norm (fig. 7 and 8) we realize that convergence rates for linear ansatz spaces remain the same as for the H^1–semi norm while for quadratic ansatz spaces the rates increase by 1.

3.2 Stability

While standard schemes for the numerical solution of (30) have a nice behaviour for large and moderate $\varepsilon \geq 1$ those schemes produce high frequent spurious solution for the singularly perturbed case $\varepsilon \ll 1$. Even if the analytical solution is bounded in most parts of the domain a single tiny characteristic or boundary layer causes the pollution of the solution in the hole domain. Since our method is based on upwinding we expect that the stability is superior to standard methods.

Boundary layers For very small ε the solution of (30) has a strong boundary layer towards the corner $(1,1)$ (fig. 9). Therefore the solution loses regularity and the convergence rates deteriorate (fig. 10). This figure shows additionally that in the case of $\mathcal{W}_1^0$ as interpolation space, upwinding can not only retain convergence outside the boundary layer, but also reduces the error substantially. The same observation can be seen for the scheme $b_h^{2b,vmb}(u_h, v_h)$ in the case of quadratic Lagrangian elements (fig. 11).

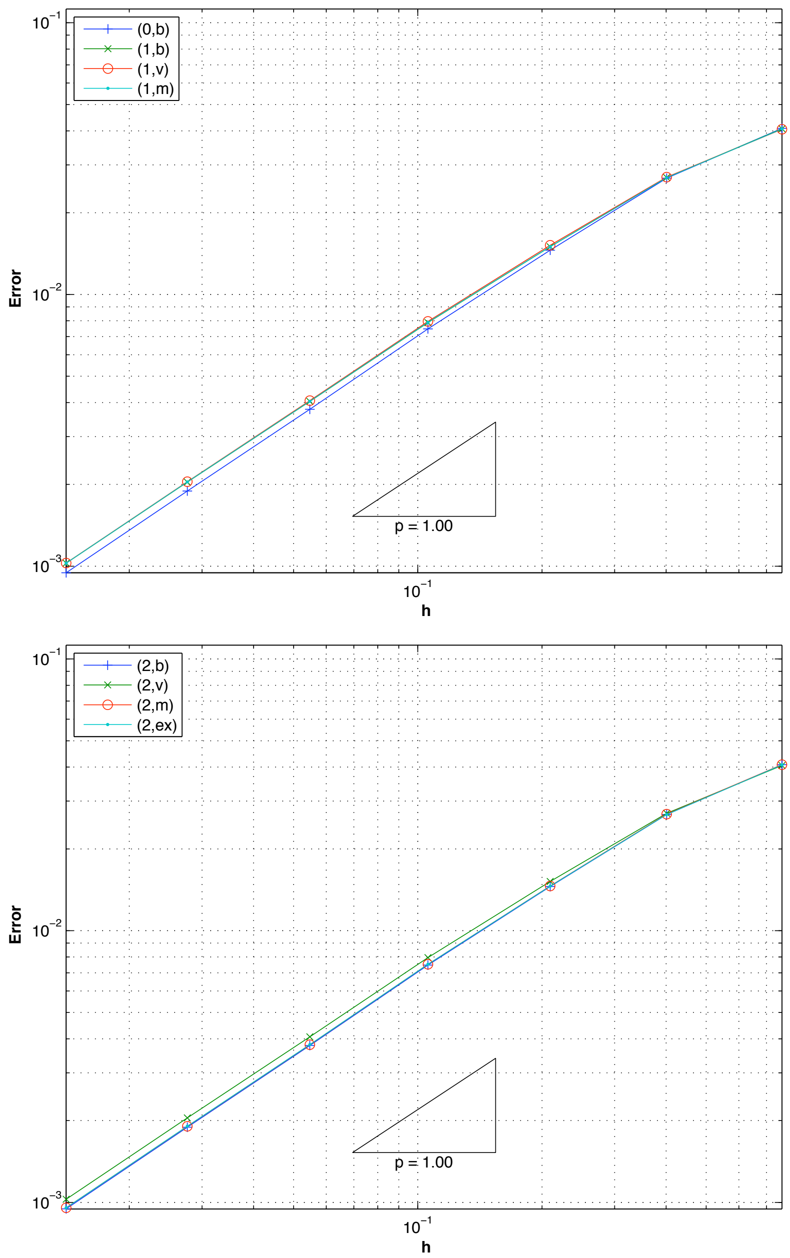

Figure 5: Convergence rate in H^1–semi norm for non perturbed problem (30) with $\varepsilon = 1$ and linear Lagrangian elements.

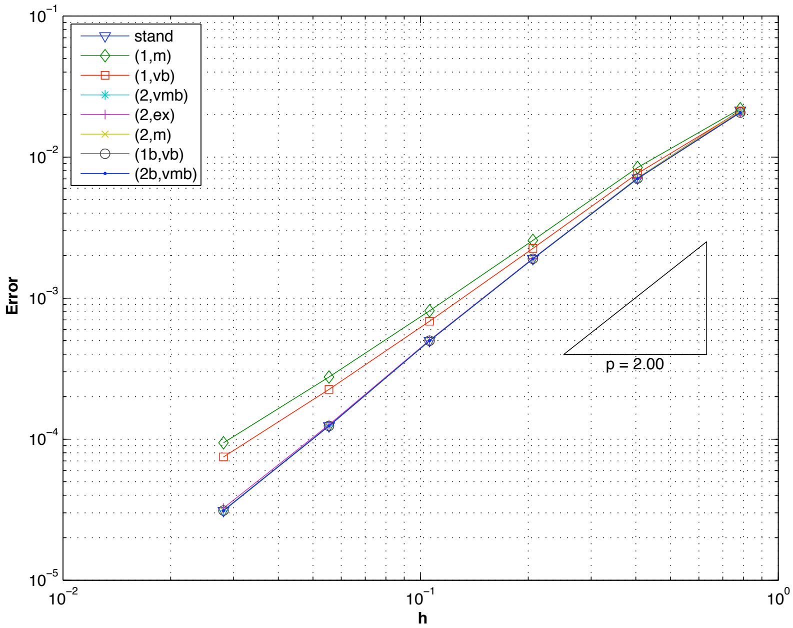

Figure 6: Convergence rate in H^1–semi norm for non perturbed problem (30) with $\varepsilon = 1$ and quadratic Lagrangian elements.

Characteristic layers To study the stability properties in presence of a characteristic layer we look at the following problem:

$$\begin{aligned} -\varepsilon\Delta u + v_1(\theta)\partial_x u + v_2(\theta)\partial_y u &= 0 \quad \text{in} \quad [0,1]^2 \\ u(x,y) &= \begin{cases} 0 & x \leq 0.5 \\ 1 & x > 0.5 \quad \text{in} \quad \partial[0,1]^2, \end{cases}, \end{aligned} \tag{32}$$

where $\boldsymbol{v}(\theta) = (cos(\theta), sin(\theta))^T$. We calculate the solutions on a regular mesh (mesh width $= 0.04$) for various θ-values $0 < \theta < \pi$ and monitor the profile of the solutions on the line running through $(0.5, 0.5)$ perpendicular to the flow. The profile lines in figure (12) indicate that the scheme using $b_h^{2b,vmb}(u_h, v_h)$ as stable as a SUPG method [6] independent of the orientation of the mesh, while the schemes using $b_h^{2,m}(u_h, v_h)$ or $b_h^{1b,vm}(u_h, v_h)$ are unstable.

3.3 Numerical prediction of stability

A more general method to predict the stability of a scheme, than just solving model problems is described in [21].G. Sangalli shows there that the solution of problem (16) fulfils

$$\lim_{\varepsilon\to 0^+} \inf_{f\in L^2(\Omega)} \frac{\|f\|_{L^2(\Omega)}}{\|\boldsymbol{\beta}\cdot\boldsymbol{\nabla} u\|_{L^2(\Omega')}} = 1,$$

where $\Omega' \subset \Omega$ with nonzero distance to the outflow boundary. He suggests that stabilization effect of a numerical method can be studied in computing the

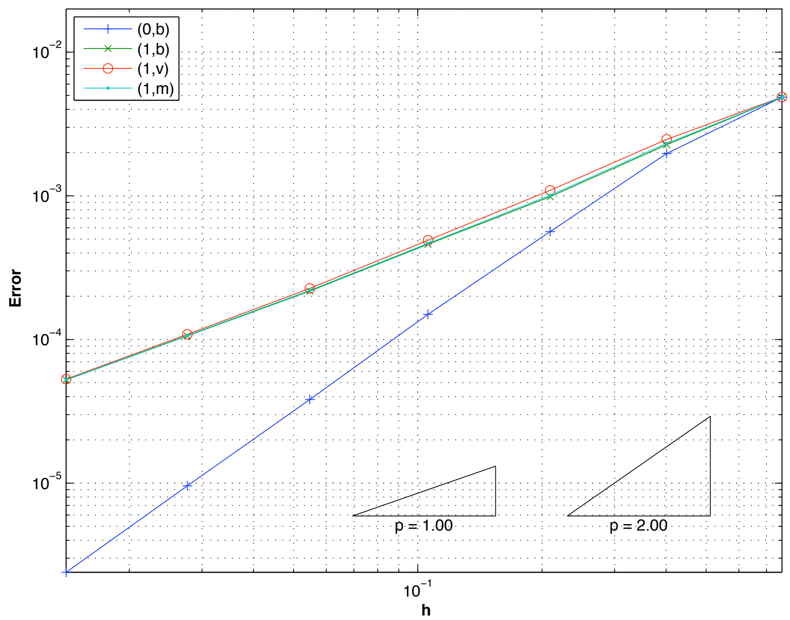

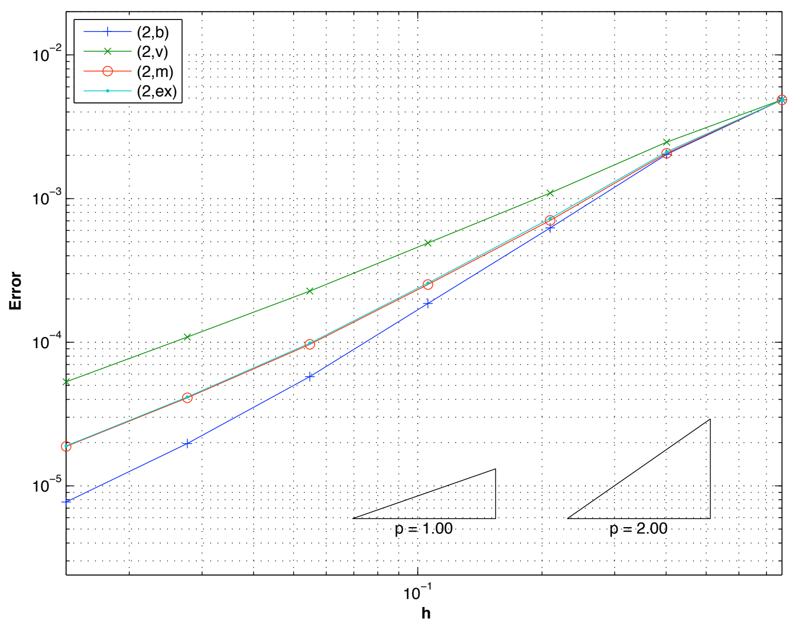

Figure 7: Convergence rate in L^2–norm for non perturbed problem (30) with $\varepsilon = 1$ and linear Lagrangian elements.

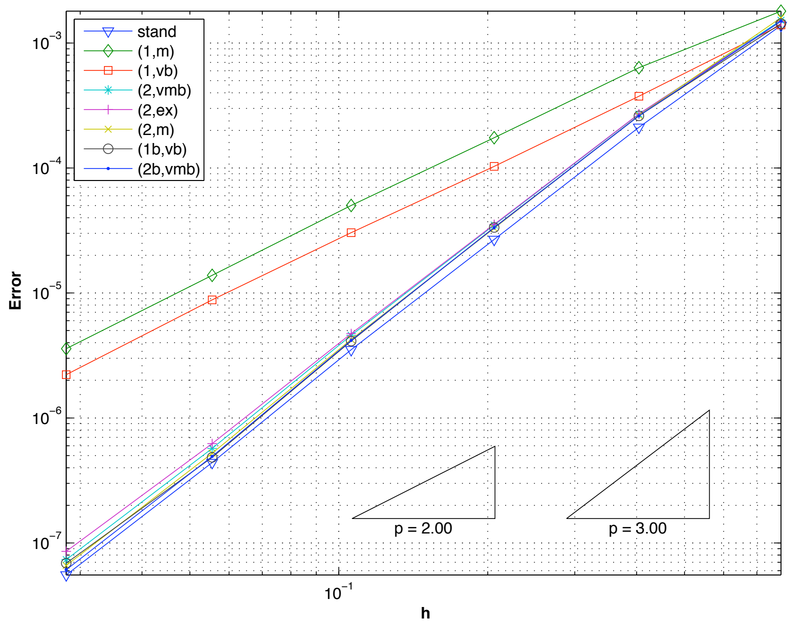

Figure 8: Convergence rate in L^2–norm for non perturbed problem (30) with $\varepsilon = 1$ and quadratic Lagrangian elements.

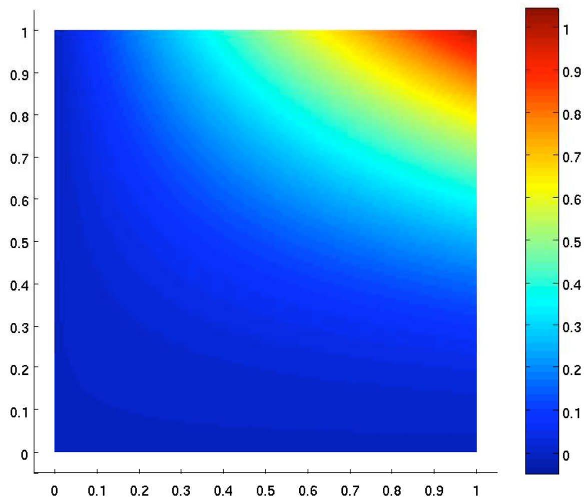

Figure 9: Analytic solution u of (30) for $\varepsilon = 10^{-10}$. Since u has homogeneous boundary conditions there occurs a boundary layer towards $(1, 1)$.

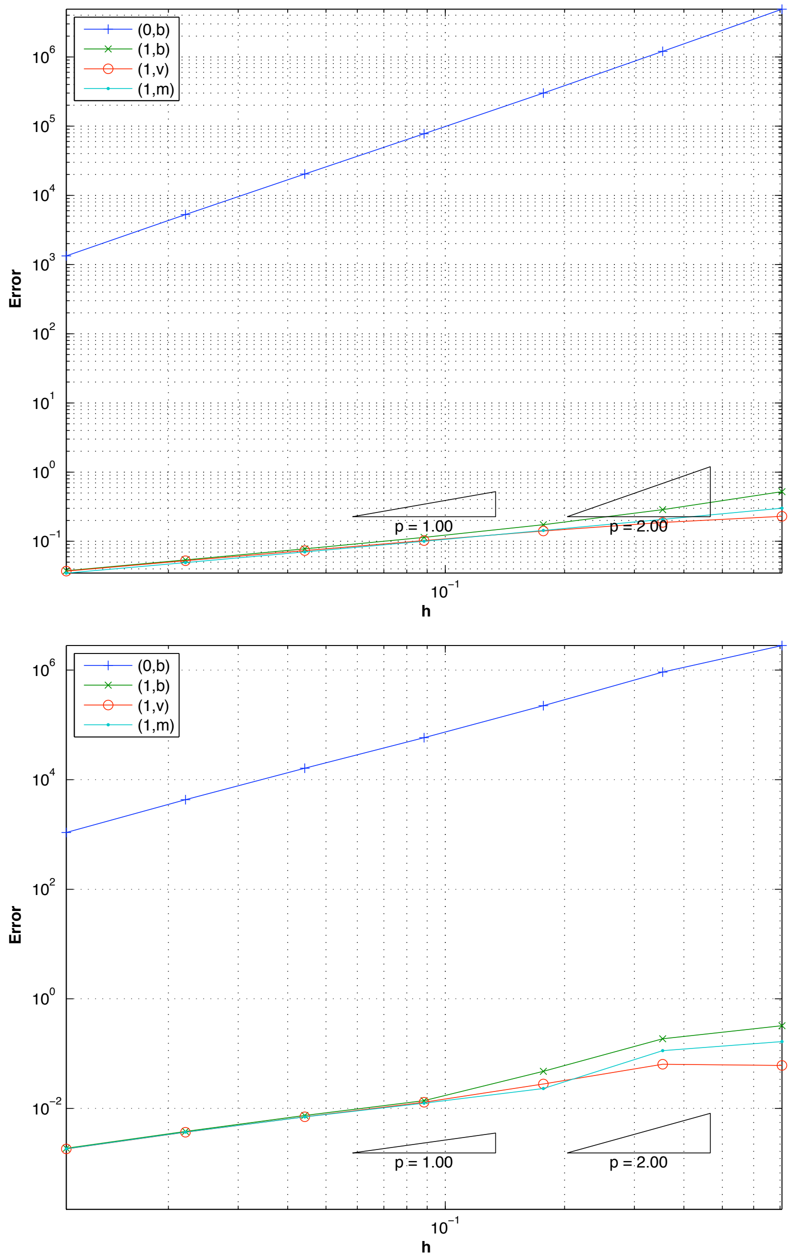

Figure 10: Convergence rate in L^2–norm for singular perturbed problem (30) with $\varepsilon = 10^{-8}$ calculated on the hole domain (upper) and on a subdomain excluding the boundary layer (linear Lagrangian elements).

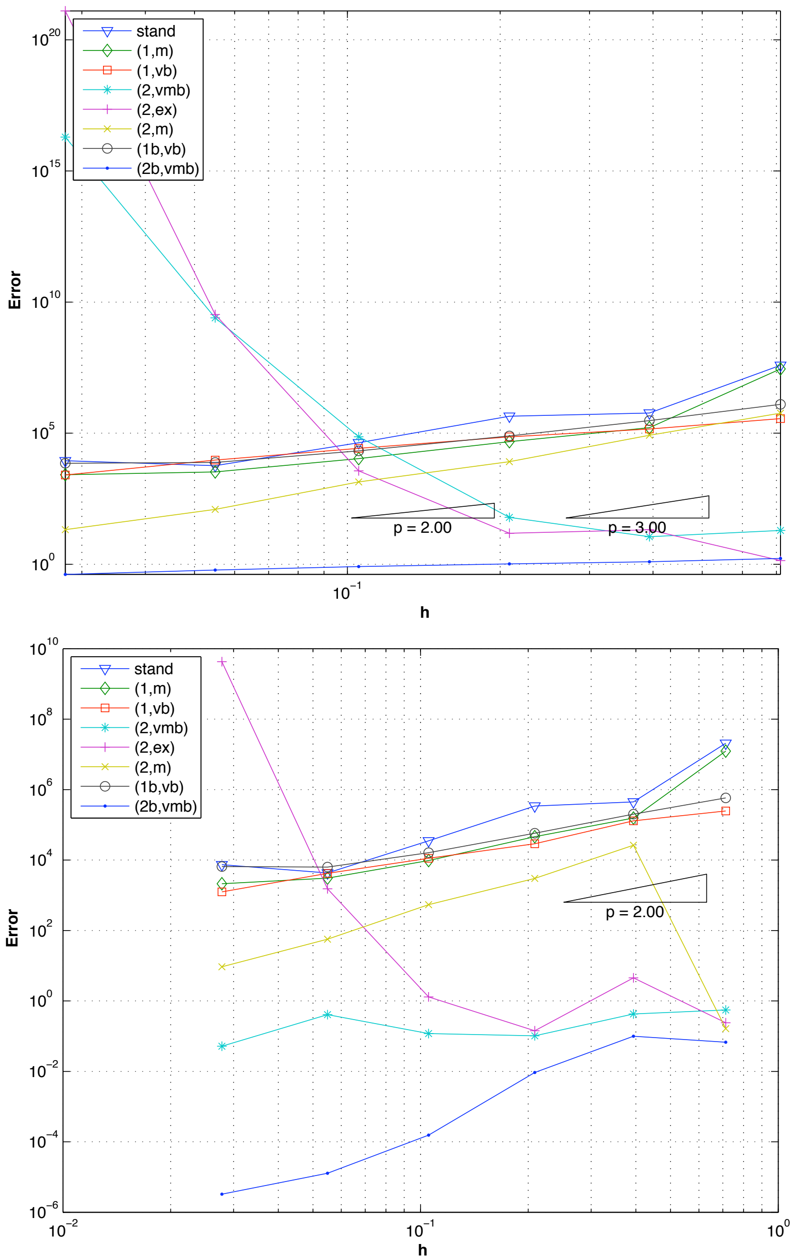

Figure 11: Convergence rate in L^2–norm for singular perturbed problem (30) with $\varepsilon = 10^{-8}$ calculated on the hole domain (upper) and on a subdomain excluding the boundary layer (quadratic Lagrangian elements).

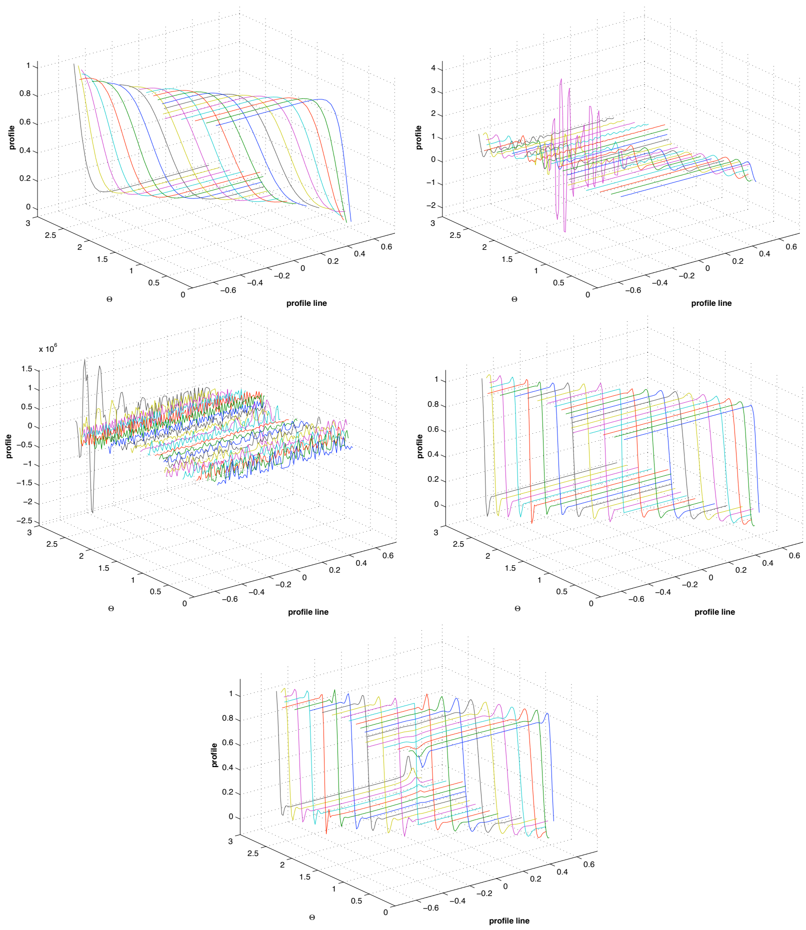

Figure 12: Profiles of the solutions of problem (32) for varying θ using the schemes with $b_h^{1,v}$, $b_h^{2,m}$, $b_h^{1b,vb}$, $b_h^{2b,vmb}$ and a SUPG implementation (left to right, top to bottom) for quadratic Lagrangian elements.

discrete counterpart:

$$s(\varepsilon) := \inf_{f \in L^2(\Omega)} \frac{\|f\|_{L^2(\Omega)}}{\|\boldsymbol{\beta} \cdot \boldsymbol{\nabla} u_h\|_{L^2(\Omega')}}. \tag{33}$$

This implies the computation of a discrete infsup-constant:

$$s(\varepsilon) = \inf_{u_h \in \mathcal{W}^0} \sup_{v_h \in \mathcal{W}^0} \frac{a(u_h, v_h) + b_h(u_h, v_h)}{\|v_h\|_{L^2(\Omega)} \|\boldsymbol{\beta} \cdot \boldsymbol{\nabla} u_h\|_{L^2(\Omega')}}, \tag{34}$$

which in turn is equivalent to a generalized eigenvalue problem:

$$S^T V^{-1} S \boldsymbol{x} = \lambda U \boldsymbol{x},$$

where S, V and U are the matrix operators for $a(u_h, v_h) + b_h(u_h, v_h)$, $(u_h, v_h)_\Omega$ and $(\boldsymbol{\beta} \cdot \boldsymbol{\nabla} u_h, \boldsymbol{\beta} \cdot \boldsymbol{\nabla} v_h)_{\Omega'}$. Then $s(\varepsilon) = \sqrt{\lambda_{min}}$ and the scheme will produce spurious oscillations, in case $s(\varepsilon)$ is close to zero.

Remark 3.1 *In the case of linear Lagrangian ansatz and interpolation spaces and local quadrature Q_c that preserves the rank of the local mass matrix, we have that*

$$b_h^{0,c}(u_h, I_0^0(\boldsymbol{\beta} \cdot \nabla u_h)) \cong \|\boldsymbol{\beta} \cdot \nabla u_h\|_{L^2(\Omega)}$$

hence $s(0) > 0$. No spurious oscillations may appear.

Figures (13) and (14) show the dependence of s on the mesh size and the diffusion constant for linear Lagrangian elements; figure 15) deals with the quadratic case. For linear Lagrangian elements and linear interpolation any upwind scheme seems to produce a non-zero value for s (fig. 13). With quadratic ansatz spaces this this is true only for $b_h^{2b,vmb}(u_h, v_h)$ (fig. 15).

4 Upwind quadrature as penalty-term formulation

Let us finally stress, that the *upwind quadrature* formulation (23) resembles a stabilized Discontinuous Galerkin methods using penalty terms. The difference between standard methods (21) and the upwind quadrature is the evaluation of the gradient at element boundaries. If we add and subtract to (23) the non-upwind quadrature evaluation and collect the different terms belonging to quadrature points we get:

$$\begin{aligned} b_h(u_h, v_h) &= \sum_T \sum_{i=1}^N \omega_i^T (\boldsymbol{\beta} \cdot \boldsymbol{\nabla} u_h)(\boldsymbol{x}_i^T) v_h(\boldsymbol{x}_i^T) \\ &\quad - \sum_T \sum_{i=1}^N \omega_i^T \left((\boldsymbol{\beta} \cdot \boldsymbol{\nabla} u_h)|_{T_i} - \boldsymbol{\beta} \cdot \boldsymbol{\nabla} u_h \right) (\boldsymbol{x}_i^T) v_h(\boldsymbol{x}_i^T) \\ &= b_h^s(u_h, v_h) + B(u_h, v_h) \end{aligned}$$

where $B(u_h, v_h)$ penalizes the jump $[\boldsymbol{\beta} \cdot \boldsymbol{\nabla} u_h]_{\boldsymbol{x}_i} := \left((\boldsymbol{\beta} \cdot \boldsymbol{\nabla} u_h)|_{T_i} - \boldsymbol{\beta} \cdot \boldsymbol{\nabla} u_h \right) (\boldsymbol{x}_i)$ at the quadrature points $\mathbf{x}_i$. The upwind quadrature enforces weak continuity of the streamline derivative $\boldsymbol{\beta} \cdot \boldsymbol{\nabla} u_h$. Unfortunately the penalty term is not symmetric like the edge penalty term in [8] and can not be used to define a mesh dependent norm.

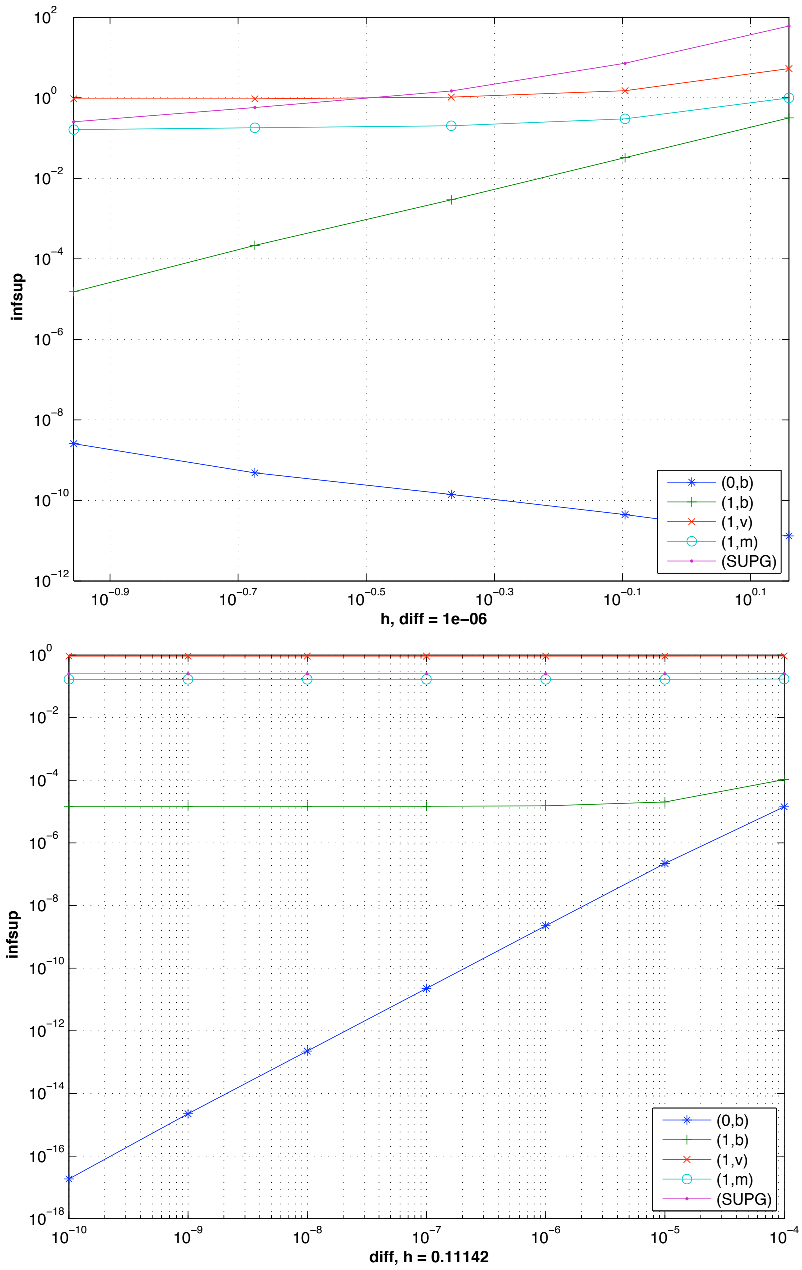

Figure 13: Numerical evaluation of $s = \textbf{infsup}$ (see (33)) for linear Lagrangian elements and linear interpolation. Upper: mesh size dependence for fixed $\varepsilon =$ diff. Lower: dependence on diffusion constant for fixed mesh size h.

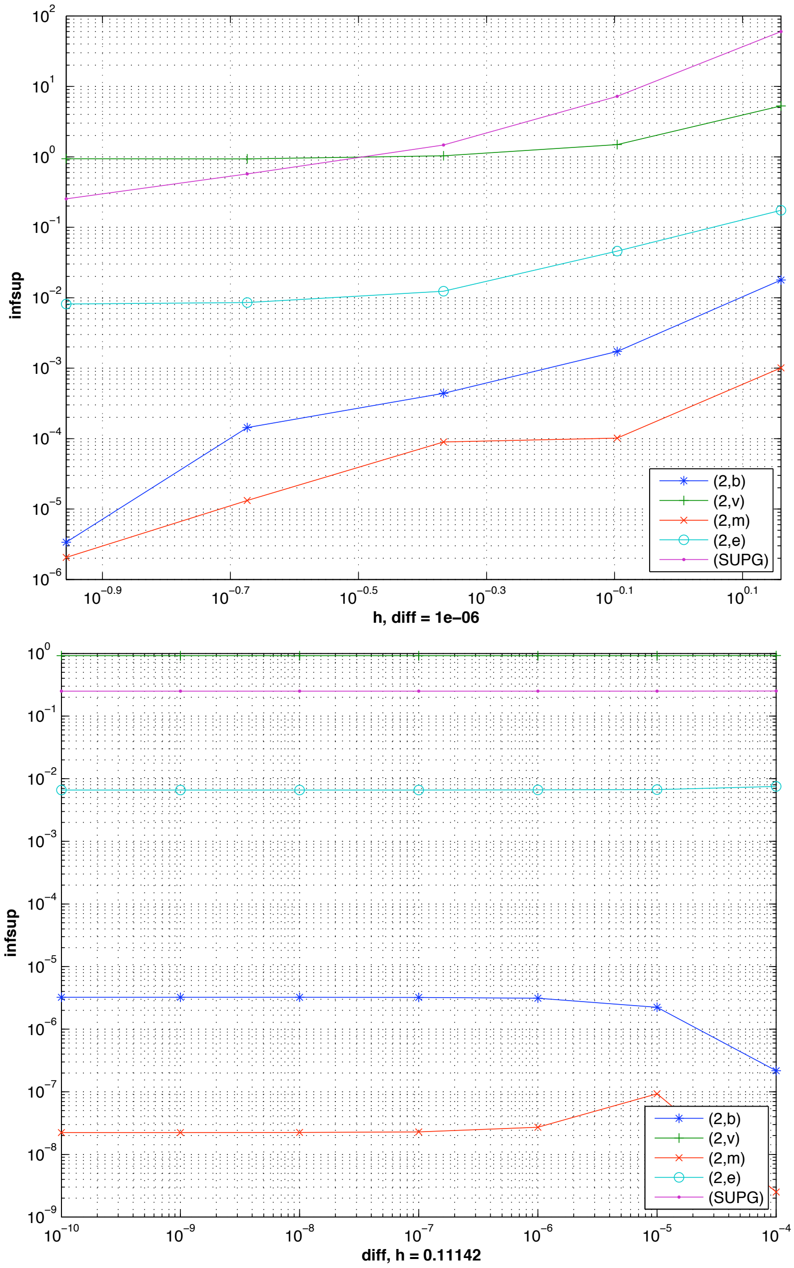

Figure 14: Numerical evaluation of $s = \mathbf{infsup}$ (see (33)) for linear Lagrangian elements and quadratic interpolation. Upper: mesh size dependence for fixed $\varepsilon = \text{diff}$. Lower: dependence on diffusion constant for fixed mesh size h.

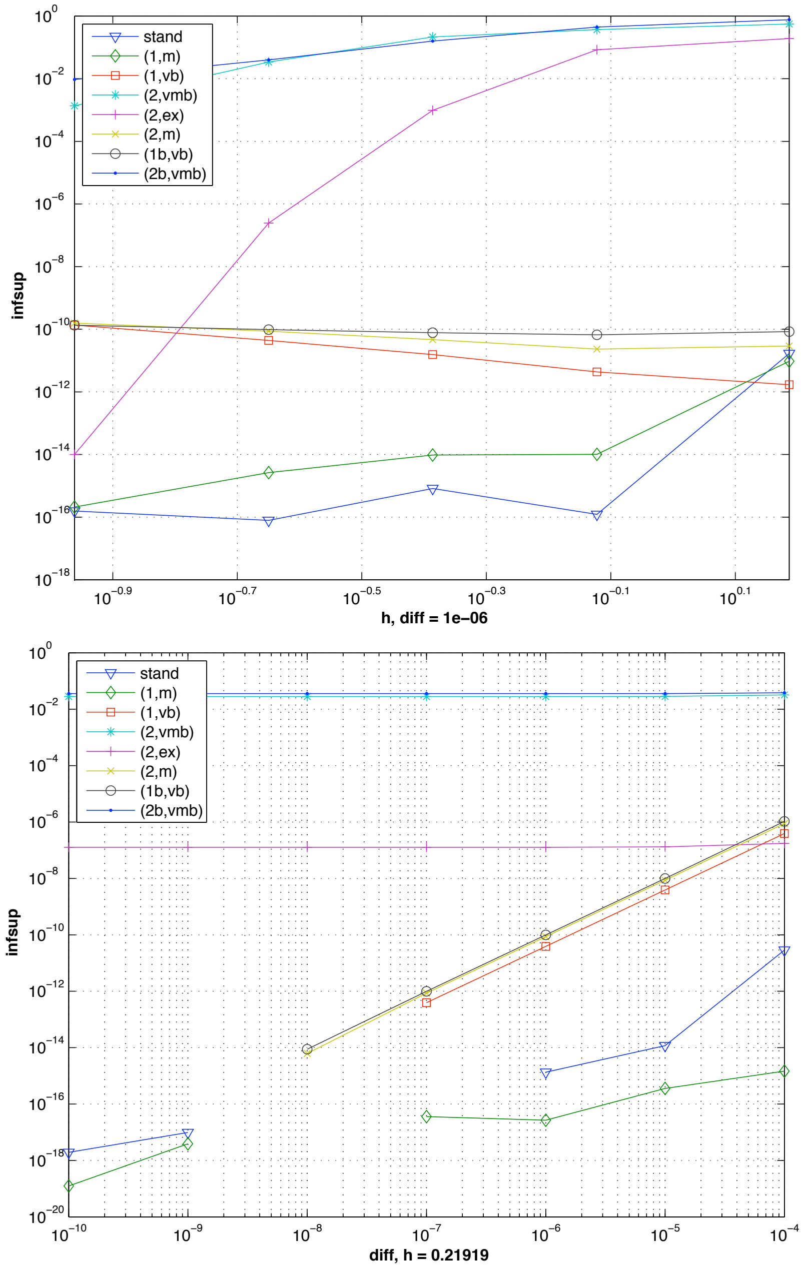

Figure 15: Numerical evaluation of s = **infsup** (see (33)) for quadratic Lagrangian elements. Upper: mesh size dependence for fixed ε = diff. Lower: dependence on diffusion constant for fixed mesh size h.

5 Conclusion

At least in some cases the proposed approximation technique based on contraction extrusion seems to lead to schemes with superior stability properties. While for linear Lagrangian elements we obtain many different stable schemes, there was only one in the quadratic case. Although this observation is confirmed by the quite general evaluation technique proposed by Sangalli [21] further research will focus on non-empirical methods to predict stability. Moreover, it is important to study the stability of schemes for differential l-forms with $l > 0$.

References

[1] Mark Ainsworth and Joe Coyle. Hierarchic finite element bases on unstructured tetrahedral meshes. *International Journal for Numerical Methods in Engineering*, 58:2103–2130, 2003.

[2] D.N. Arnold, R.S. Falk, and R. Winther. Finite element exterior calculus, homological techniques, and applications. *Acta Numerica*, 15:1–155, 2006.

[3] Alain Bossavit. Applied differential geometry.

[4] Alain Bossavit. Extrusion, contraction: their discretization via Whitney forms. *The International Journal for Computation and Mathematics in the Electrical and Electronic Engineering*, 22(2):470–480, 2003.

[5] Alain Bossavit. Discretization of electromagnetic problems: The "generalized finite differences". In W.H.A. Schilders and W.J.W. ter Maten, editors, *Numerical Methods in Electromagnetics*, volume XIII of *Handbook of numerical analysis*, pages 443–522. Elsevier, Amsterdam, 2005.

[6] Alexander N. Brooks and Thomas J.R. Hughes. Streamline upwind/Petrov-Galerkin formulations for convection dominated flows with particular emphasis on incompressible Navier-Stokes equations. *Computer Methods Applied Mechanics Engineering*, 32:199–259, 1982.

[7] Eric Burman. A unified analysis for conforming and nonconforming stabilized finite element methods using interior penalty. *SIAM J. Numer. Anal.*, 43(5):2012–2033, 2005.

[8] Eric Burman and Peter Hansbo. Edge stabilization for Galerkin approximations of convection-diffusion-reaction problems. *Computer Methods Applied Mechanics Engineering*, 193:1437–1453, 2004.

[9] Erik Burman and Alexandre Ern. Discrete maximum principle for Galerkin approximations of the Laplace operator in arbitrary meshes. *Numerical Analysis*, 338:641–646, 2004.

[10] P.G. Ciarlet. *Handbook of Numerical Analysis, Vol II*, chapter Basic Error Estimates for Elliptic Problems, pages 18–351. Elsvier Science Publisher B.V. (North-Holland), 1991.

[11] Ralf Hiptmair. Canonical construction of finite elements. *Math. Comp.*, 68:1325–1346, 1999.

[12] Ralf Hiptmair. Discrete Hodge operators. *Numerische Mathematik*, 90:265–289, 2001.

[13] Ralf Hiptmair. Finite elements in computational electromagnetism. *Acta Numerica*, 11:237–339, 2002.

[14] T.J.R. Hughes, L.P. Franca, and G.M. Hulbert. A new finite element formulation for computational fluid dynamics: VIII The Galerkin/Least-Squares method for advective diffusive equations. *Computer Methods Applied Mechanics Engineering*, 73:173–189, 1989.

[15] Tsutomu Ikeda. *Maximum Principle in Finite Element Models for Convection–Diffusion Phenomena*. North-Holland, 1983.

[16] Serge Lang. *Fundamentals of Differential Geometry*. Springer, 1999.

[17] Jens Lorenz. Zur Inversmonotonie diskreter Probleme. *Numerische Mathematik*, 27:227–238, 1977.

[18] Akira Mizukami and Thomas J.R. Hughes. A Petrov-Gialerkin finite element method for convection-dominated flows: An accurate upwinding technique for satisfying the maximum principle. *Computer Methods in Applied Mechanics and Engineering*, 50:181–193, 1985.

[19] H.G. Roos. A second order monotone upwind scheme. *Computing*, 36(1-2):57–67, 1986.

[20] H.G. Roos, M. Stynes, and L. Tobiska. *Numerical Methods for Singular perturbed Differential Equations*. Springer, 1996.

[21] G. Sangalli. Numerical evaluation of finite element methods in convection diffusion problems. *CALCOLO*, 37:233–255, 2000.

[22] M. Tabata. A finite element approximation corresponding to the upwind finite differencing. *Mem. Numer. Math.*, 4:47–63, 1977.

[23] Harry Yserentant. Die maximale Konsistenzordnung von Differenzenapproximationen nichtnegativer Art. *Numerische Mathematik*, 42:119–123, 1983.

Research Reports

No.	Authors	Title
08-30	H. Heumann, R. Hiptmair	Extrusion contraction upwind schemes for convection-diffusion problems
08-29	N. Hilber, C. Schwab, C. Winter	Variational sensitivity analysis of parametric Markovian market models
08-28	K.Schmidt, S. Tordeux	Asymptotic modelling of conductive thin sheets
08-27	R. Hiptmair, P.R. Kotiuga, S. Tordeux	Self-adjoint curl operators
08-26	N. Reich	Wavelet compression of anisotropic integro-differential operators on sparse tensor product spaces
08-25	N. Reich	Anisotropic operator symbols arising from multivariate jump processes
08-24	N. Reich	Wavelet compression of integral operators on sparse tensor spaces: Construction, Consistency and Asymptotically Optimal Complexity
08-23	F. Liu, N. Reich and A. Zhou	Two-scale finite element discretizations for infinitesimal generators of jump processes in finance
08-22	M. Bieri and Ch. Schwab	Sparse high order FEM for elliptic sPDEs
08-21	M. Torrilhon and R. Jeltsch	Essentially optimal explicit Runge-Kutta methods with application to hyperbolic-parabolic equations
08-20	G. Dahlquist and R. Jeltsch	Generalized disks of contractivity for explicit and implicit Runge-Kutta methods
08-19	M. Karow and D. Kressner	On the structured distance to uncontrollability
08-18	D. Kressner, Ch. Schroeder and D.S. Watkins	Implicit QR algorithms for palindromic and even eigenvalue problems
08-17	B. Kagstroem, D. Kressner, E.S. Quintana-Ort and G. Quintana-Ort	Blocked algorithms for the reduction to Hessenberg-Triangular form revisited